Calculs Automatiques à une Boucle dans la Théorie électrofaible

Fawzi BOUDJEMA
LAPTH, CNRS, France

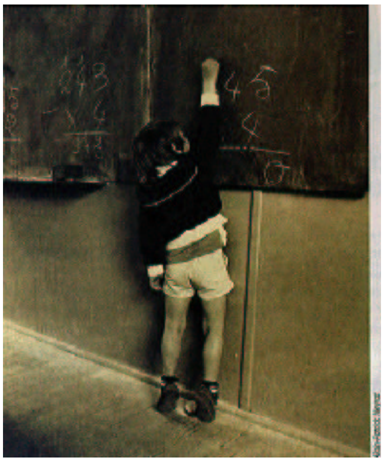

for the GRACE-Loop Collaboration
LAPTH (Annecy) & Minami-Tateya (KEK)

based on

- hep-ph/0308080, (Phys. Rep.) Grace-loop and set up for these calculations
- hep-ph/0211268 (Nucl.Phys.Proc.Suppl.116,2003) and hep-ph/0212261 (PLB559:252,2003) Single Higgs Production
- hep-ph/0307029 (PLB571:163,2003) $t\bar{t}H$
- hep-ph/0309010 (PLB576:152,2003) ZHH
- in Progress e^+e^-H and ...

Application à SUSY (à l'arbre): Calcul de densité relique
G. Bélanger, FB, S. Pukhov and A. Semenov

- Comput.Phys.Commun.149:103-120,2002.
- JHEP 0403:012,2004.

Application à SUSY (boucle) et MS (encore plus d'automatisation)
FB, A. Semenov and D. Temes

Historique des calculs en boucles en EW

- Fin des années 80:
calculs pour la physique du LEP 1.
En grande partie calculs à une boucle pour $Z \to f\bar{f}$
ceci a pris plusieurs années et a impliqué plusieurs groupes
Principalement des fonctions à 2-point et 3-points (qq 4-points).
Quelques dizaines de diagrammes.

- début années 90:
calculs pour la physique du LEP 2.
3 ans pour $e^+e^- \to W^+W^-$ (Leiden-Wurzburg)

- Année 95 (LEP2 WG):
6 mois pour inclure le calcul de boites pour production de b!

- Début années 2000 :
Calcul de précision pour le LC

Calculs électrofaibles vs calculs QCD (perturbative)

EW: Un assez grand nombre de particules
EW: Plusieurs masses et plusieurs échelles
EW: renormalisation plus complique
EW: pratiquement impossible d'arriver à des résultats compactes
(seulement pour des processus type QED: $Z \to 3\gamma, \gamma\gamma \to \gamma\gamma$)
EW: Infra-rouge plus simple.

: Largeur!

The LC will be a machine for *precision* measurements in particular ♡ the HIGGS →: Prime motivation.

Lot of work (theory) and (experiment) done on branching ratios (and mass) measurements

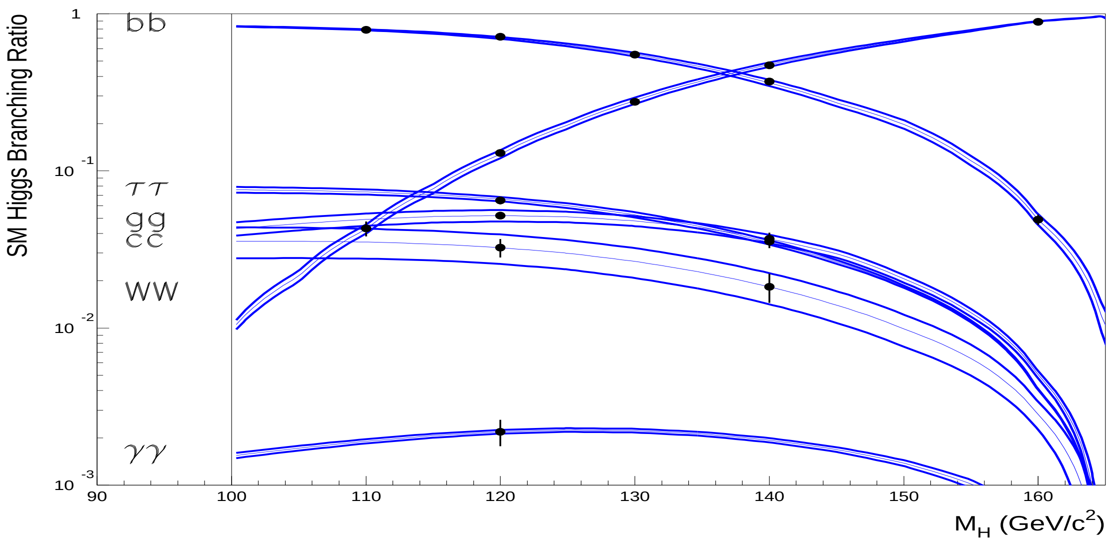

Until the last few months, the main production mechanisms were not known with an accuracy that matches the experimental precision!

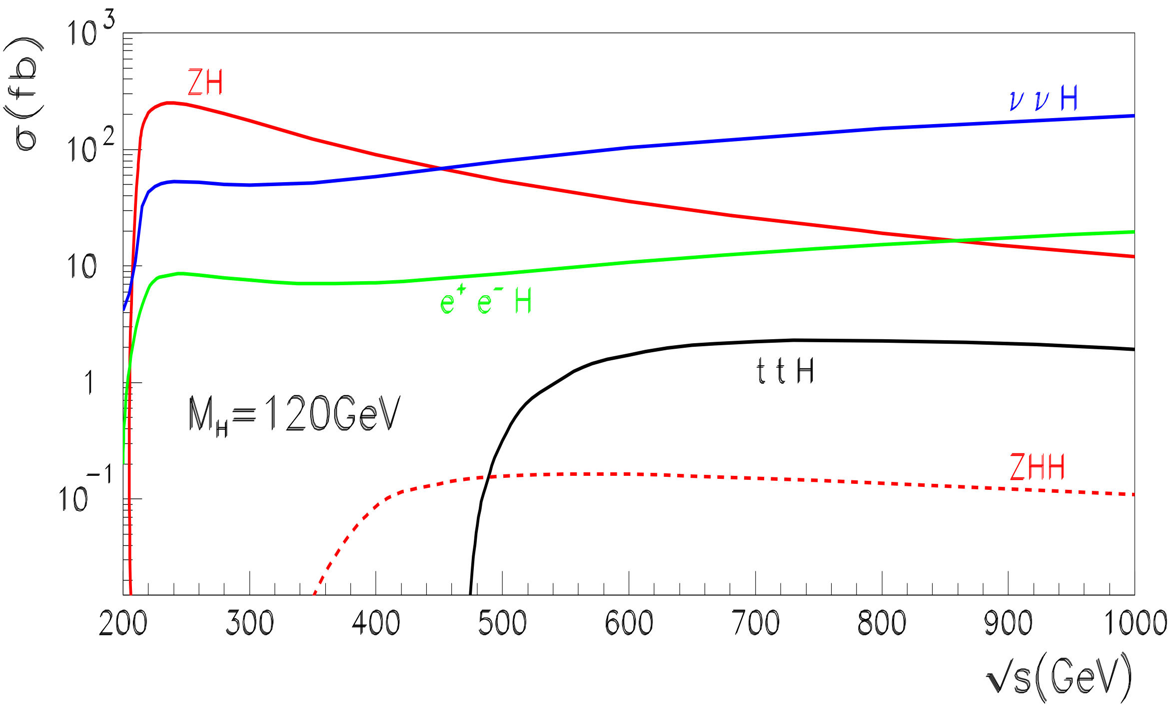

- *The difficulty is that all these processes are* $2 \to 3$ *processes. For instance no analytical formulae known for the total cross section* $e^+e^- \to \nu\bar{\nu}H$ $\left(\sigma(e^+e^- \to \nu\bar{\nu}H) > \sigma(e^+e^- \to ZH)\right.$.
- *interference* ZH-$\nu\bar{\nu}H$ *at tree-level only achieved in 1996.*
- *Single H determines* HWW,..

$t\bar{t}H$ and ZHH are both very important for the overall Higgs profile, but cross sections are small

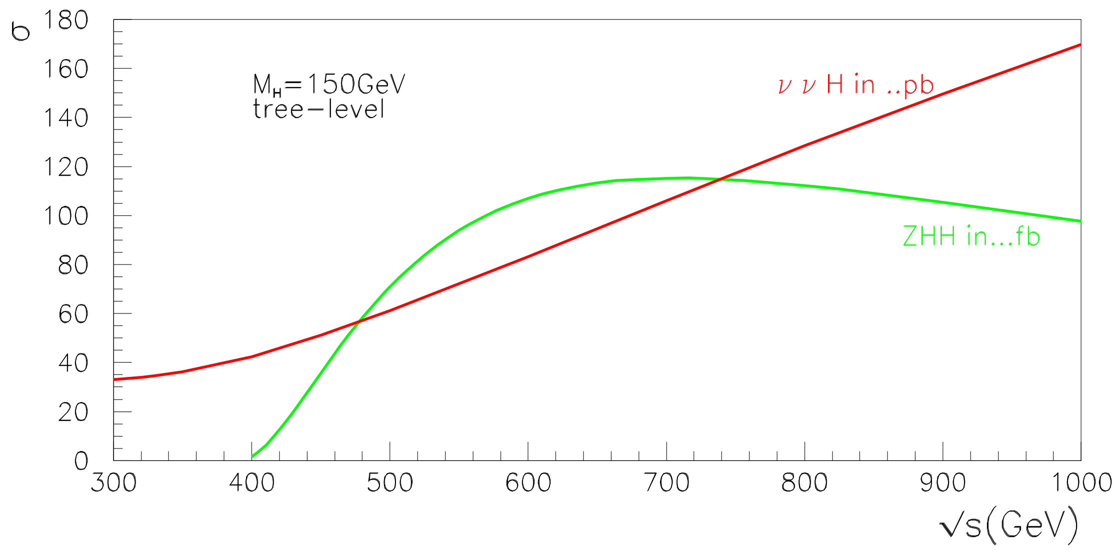

so what's at stake, sudying these low-yield processes?

The Higgs Potential

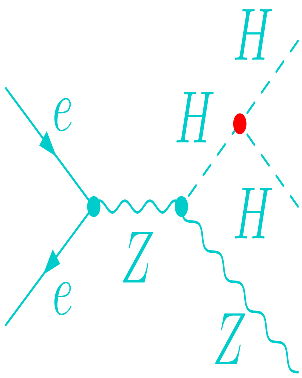

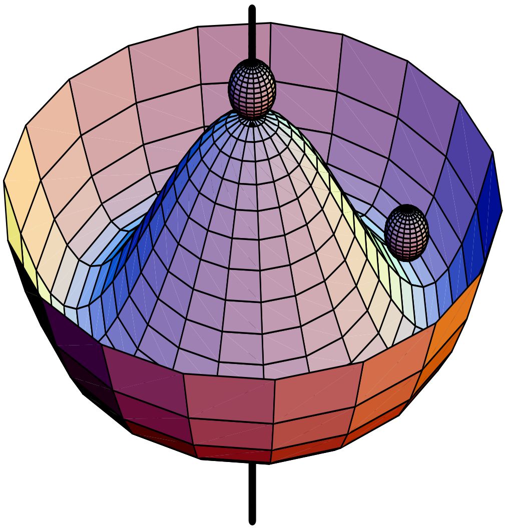

Deviations in the "SM" Higgs potential, FB+Chopin 95, FB+Semenov 02

$$V_{\mathcal{SSB}} = \lambda \left\{ \sum_{n=2} \frac{g^{2(n-2)}}{\Lambda^{2(n-2)}} \frac{a_n}{(n-1)^2} \left[\Phi\ \Phi - \frac{v^2}{2} \right]^n \right\}$$

$$\begin{aligned} V_{\mathcal{SSB}} &= \frac{1}{2} M_H^2 \left\{ H^2 + \frac{g}{M_W} H(\varphi^+\varphi^- + \frac{\varphi_3^2}{2}) + \frac{g}{2M_W} h_3 H^3 \right. \\ &\left. h_4 \left(\frac{g}{4M_W} \right)^2 H^4 + h_3' \left(\frac{g}{2M_W} \right)^2 H^2(\varphi^+\varphi^- + \frac{\varphi_3^2}{2}) \ldots\ldots \right\} \end{aligned}$$

$$\begin{aligned} h_3 &= 1 + a_3 \frac{M_W^2}{\Lambda^2} = 1 + \delta h_3 \\ h_4 &= 1 + 6\delta h_3 \\ h_3' &= 1 + 3\delta h_3 \end{aligned}$$

$$\lambda_{HHH} = \lambda_{HHH}^0 \left(1 - \frac{\alpha}{\pi s_W^2} \frac{M_t^4}{M_W^2 M_H^2} \right),$$

Amounts to 10% correction in the coupling (for $M_H = 120$GeV) which is the experimental precision.!

Top is special

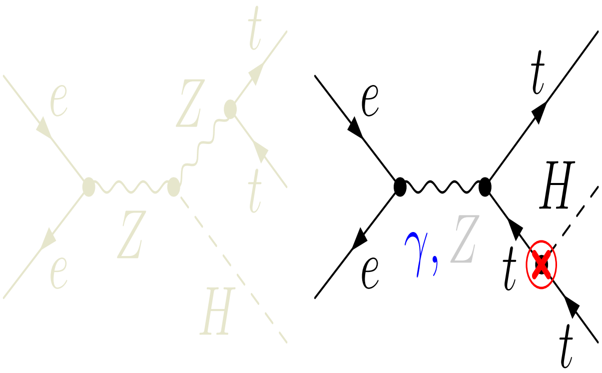

A probe into the $t\bar{t}H$ Yukawa coupling

⋆ unconventional mechanisms of symmetry breaking

• topcolor

♢ little Higgs

$$- \mathcal{L}^l_m = \sum_{i=e,\mu,\tau} y^i_l \left(\bar{L}_i \Phi l_{R,i} + \bar{l}_{R,i} \Phi\ L_i\right) \longrightarrow \text{unitary gauge} \longrightarrow$$

$$\sum_{i=e,\mu,\tau} \frac{y^i_l v}{\sqrt{2}} \left(1 + \frac{H}{v}\right) \bar{l}_i l_i \ , \ \frac{y^i_l v}{\sqrt{2}} = m^i_l.$$

The top Yukawa coupling is large

$y_t \sim 1$ **and** $\lambda_t = y_t^2/4\pi \sim \alpha_s(m_t)$

experimental precision is 5% **then**

RC important

Theoretical challenge

Computation is challenging and increase in complexity (at least in size) as we seek to probe processes with smaller cross section

Huge number of diagrams.....with a non-negligible number of pentagons.

	tree	one-loop
ZH	1	82
	(3)	(341)
$\nu_e\bar{\nu}_e H$	2	249
	(12)	(1350)
e^+e^-H	2	510
	(42)	(4470)
$t\bar{t}H$	6	758
	(12)	(2327)
ZHH	6	1597
	(27)	(5417)
$\nu_e\bar{\nu}_e\gamma$	5	331
	(10)	(1099)

(..) keeping the electron Yukawa coupling.

Loop Integrals and Reduction

$$T^{(N)}_{\underbrace{\mu\nu\cdots\rho}_{M}} = \int \frac{d^n l}{(2\pi)^n} \frac{l_\mu l_\nu \cdots l_\rho}{D_0 D_1 \cdots D_{N-1}}, \qquad M \leq N$$

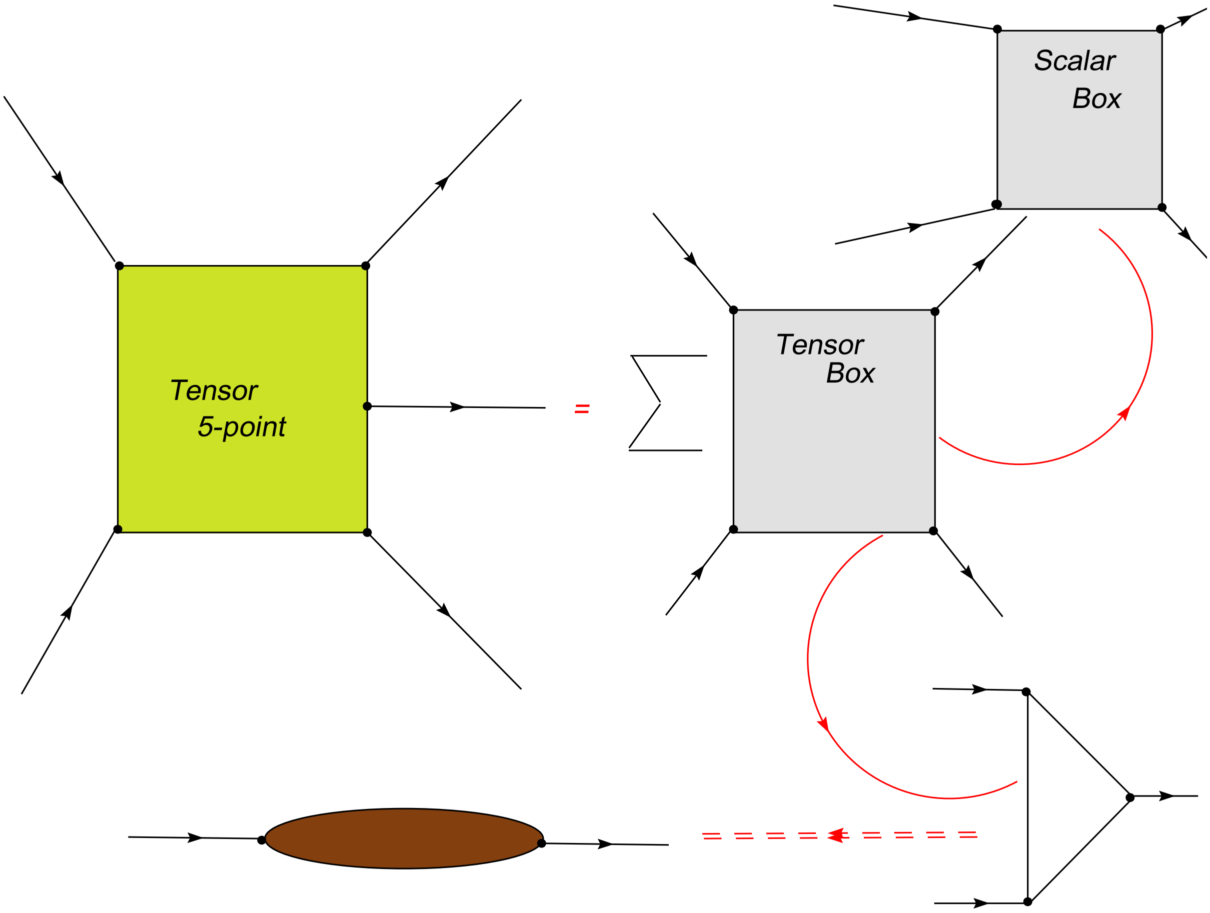

- Scalar box and triangles without γ exchange $\longrightarrow$ FF Package.
- Tensor integrals reduced to scalars using a novel procedure acting on the Feynman parameters (different from the usual Passarino-Veltman)
- ex. rank 4 box need to solve a system of 15×15 equations. In our case simplification: $15 \to 3 \bigoplus 3 \bigoplus 3 \bigoplus 6$ etc

Réduction des tenseurs en scalaires

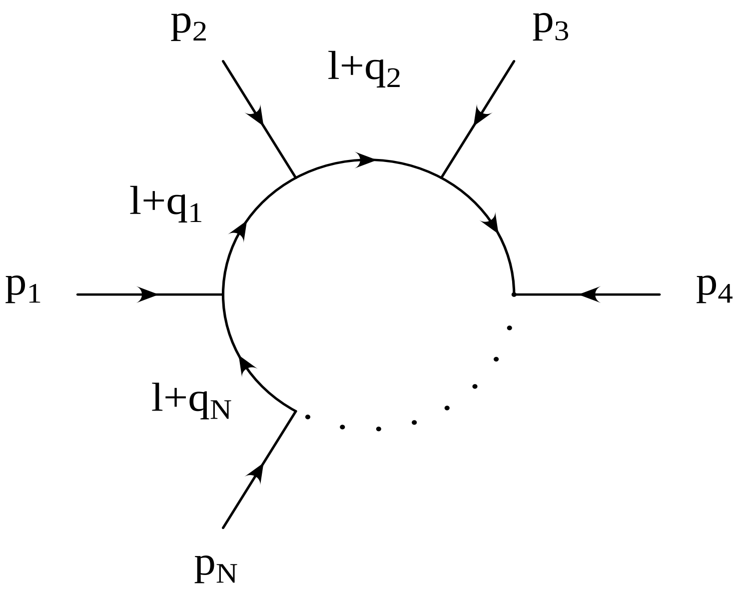

$$T^{(N)}_{\underbrace{\mu\nu\cdots\rho}_{M}} = \int \frac{d^n r}{(2\pi)^n} \frac{r_\mu r_\nu \cdots r_\rho}{D_0 D_1 \cdots D_{N-1}}, \qquad M \leq N,$$

$$D_i = (r+q_i)^2 - M_i^2, \qquad q_i = \sum_{j=1}^{i} p_j, \qquad q_0 = 0.$$

$$\frac{1}{D_0 D_1 \cdots D_{N-1}} = \int [dx] \frac{\Gamma(N)}{\left(D_1 x_1 \; + \; D_2 x_2 + \cdots D_0 (1 - \sum_{i=1}^{N-1} x_i)\right)^N}$$

$$\int [dx] = \int_0^1 dx_1 \int_0^{1-x_1} dx_2 \cdots \int_0^{1-\sum\limits_{i=1}^{N-2} x_i} dx_{N-1}.$$

$$T^{(N)}_{\underbrace{\mu\nu\cdots\rho}_{M}} = \Gamma(N) \int [dx] \, \mathcal{T}^{(N)}_{\underbrace{\mu\nu\cdots\rho}_{M}}, \quad \text{with}$$

$$\mathcal{T}^{(N)}_{\underbrace{\mu\nu\cdots\rho}_{M}} = \int \frac{d^n r}{(2\pi)^n} \frac{r_\mu r_\nu \cdots r_\rho}{(r^2 - 2r.P(x_i) - M^2(x_i))^N}, \qquad M \leq N$$

The loop momenta, over r, is done trivially.
The problem is then the integrations over the parametric integrals.

$$I^{(N)}_{\underbrace{i\cdots k}_{M}} = \int [dx] \frac{x_i \cdots x_k}{\Delta^{(N-2)}} \quad \text{and} \tag{1}$$

$$J^{(N)}_{i;\alpha} = \int [dx] x_i^\alpha \log \Delta \quad \alpha = 0, 1.$$

Solely in terms of the scalar integrals: Use FF

$$I^{(N)} = \int [dx] \Delta^{-(N-2)}$$

$$\Delta = \sum_{i,j=1}^{N-1} Q_{ij} x_i x_j + \sum_{i=1}^{N-1} L_i x_i + \Delta_0, \quad Q_{ij} = q_i.q_j,$$

$$L_i = -q_i^2 + (M_i^2 - M_0^2), \quad \Delta_0 = M_0^2 \quad P = -\sum_{i=1}^{N-1} q_i x_i$$

Example: The Boxes

15 *different integrals for the rank*-4 *box,*

10 *for the rank*-3*,*

6 *for the rank*-2 *and*

3 *for the rank*-1.

Trick

$$\overbrace{\partial_i \left(\frac{x_k^\alpha x_l^\beta x_m^\gamma}{\Delta} \right)}^{M,N-1} = -\frac{x_k^\alpha x_l^\beta x_m^\gamma}{\Delta^2} (\overbrace{L_i}^{M,N} + 2 \sum_j \overbrace{Q_{ij} x_j}^{M+1,N})$$

$$+ \frac{1}{\Delta^2} \left(\overbrace{\Delta_0}^{N,M-1} + \overbrace{\sum_j L_j x_j}^{M,N} + \sum_{jn} \overbrace{Q_{jn} x_j x_n}^{M+1,N} \right) \times$$

$$\left(\alpha x_k^{\alpha-1} x_l^\beta x_m^\gamma \delta_{ki} + \beta x_l^{\beta-1} x_k^\alpha x_m^\gamma \delta_{li} + \gamma x_m^{\gamma-1} x_k^\alpha x_l^\beta \delta_{mi} \right)$$

$$\overbrace{C_{i;klm}}^{(M,N-1),(M,N)} = -\overbrace{2\sum_j Q_{ij} I^{(4)}_{jklm} + \sum_{jn} Q_{jn}\left(\delta_{ki} I^{(4)}_{jnlm} + \delta_{li} I^{(4)}_{jnkm} + \delta_{mi} I^{(4)}_{jnkl}\right)}^{M+1,N}$$

More equations than variables! in principle good for checks but !

Finding a minimum set

$$\tilde{C}_{i;kkk} = -\frac{1}{2} \quad \left(C_{i;kkk} - \delta_{ki}\sum_i C_{i;ikk}\right) = \sum_j Q_{ij} I^{(4)}_{jkkk} \rightarrow 3 sets\ of 3\times 3$$

$$C_{i;jkk} = -2\sum_n Q_{in} I^{(4)}_{njkk}, \quad i \neq j \neq k \rightarrow 6\times 6$$

$$\sum_i C_{i;ikk} = 3\sum_{jn} Q_{jn} I^{(4)}_{jnkk}$$

$\mathbf{M=4, N=4 \rightarrow 15\times 15 = 3 \bigoplus 3 \bigoplus 3 \bigoplus 6}$
$\mathbf{M=3, N=4 \rightarrow 10\times 10 = 3 \bigoplus 3 \bigoplus 3 \bigoplus 1}$
$\mathbf{M=3, N=3 \rightarrow 4\times 4 = 2 \bigoplus 2}$
etc

For triangles and J's

$$x_i^\alpha \log\Delta_N = \frac{1}{N+\alpha-1}\sum_{j=1}^{N-1}\left\{\partial_j\left(x_i^\alpha x_j \log\Delta_N\right) - x_i^\alpha x_j \partial_j\left(\log\Delta_N\right)\right\}$$

Pentagons: Five Point Function

$$T^{(5)} = \int \frac{d^n l}{(2\pi)^n} \frac{N(l)}{D_0 D_1 \cdots D_4} = G^{\mu\nu\cdots\rho} \int \frac{d^n l}{(2\pi)^n} \frac{\overbrace{l_\mu l_\nu \cdots l_\rho}^{M}}{D_0 D_1 \cdots D_4}, \quad M \leq 5,$$

The set q_i forms a basis for vectors in 4-dimensional space

Gram matrix $A_{ij} = q_i . q_j$ then

$$\begin{aligned} g^{\mu\nu} &= \sum_{i,j=1}^{4} q_i^\mu A_{ij}^{-1} q_j^\nu, \quad l^\mu = \sum_{i,j} q_i^\mu A_{ij}^{-1} (l.q_j) \\ N(l) &= \sum_{\alpha=0}^{4} E_\alpha(l) D_\alpha + F, \end{aligned}$$

Similar trick to reduce five-point scalar to 4-point scalar.

INFRARED DIVERGENCE

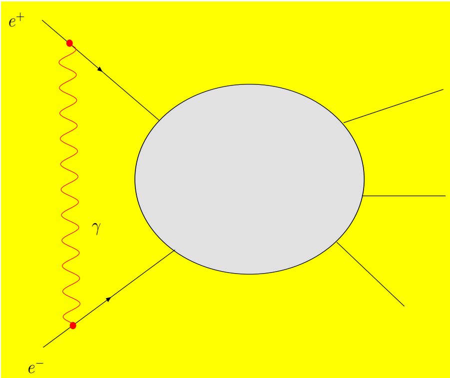

infrared divergent needs photon mass λ

$d\sigma_V(\lambda)$

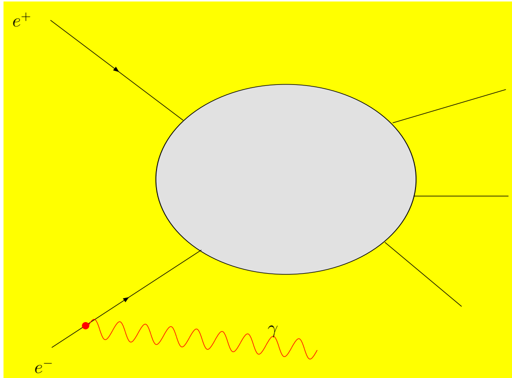

must include bremsstrahlung

$d\sigma_s(\lambda, E_\gamma < k_c) + d\sigma_H(\lambda, E_\gamma > k_c)$

$d\sigma_s \longrightarrow$ *analytical ;*

$d\sigma_H \longrightarrow$ *adaptive MC*

$$\begin{aligned}
\sigma_{\mathcal{O}(\alpha)} &= \sigma_0(1+\delta_{\mathcal{O}(\alpha)}) = \int d\sigma_0\,(1+\delta_V+\delta_S(k_c)) + \int d\sigma_H(k_c), \\
&= \underbrace{\int d\sigma_0\,\left(1+\delta_V^{EW}\right)}_{\sigma_0(1+\delta_W)} + \underbrace{\int d\sigma_0\,\left(\delta_V^{QED}+\delta_S(k_c)\right)}_{\sigma_{V+S}^{QED}(k_c)} + \underbrace{\int d\sigma_H(k_c)}_{\sigma_H(k_c)} \\
&= \sigma_0(1+\delta_W+\delta_{\rm QED}).
\end{aligned}$$

Instead of this slicing we also implement a subtraction (modeling the the collinear and infra-red singularities)

We also check against the universal factor

$$\delta_{V+S}^{QED} = \frac{2\alpha}{\pi}\left((L_e-1)\ln\frac{k_c}{E_b}+\frac{3}{4}L_e+\frac{\pi^2}{6}-1\right), \qquad L_e=\ln(s/m_e^2)\,,$$

QED corrections: Slicing *vs* subtracting, k_c check

Slicing

$$\begin{aligned}
\sigma_{\mathcal{O}(\alpha)} &= \sigma_0(1+\delta_{\mathcal{O}(\alpha)}) = \int d\sigma_0\,(1+\delta_V+\delta_S(k_c)) + \int d\sigma_H(k_c), \\
&= \underbrace{\int d\sigma_0\,(1+\delta_V^{EW})}_{\sigma_0(1+\delta_W)} + \underbrace{\int d\sigma_0\left(\delta_V^{QED}+\delta_S(k_c)\right)}_{\sigma_{V+S}^{QED}(k_c)} + \underbrace{\int d\sigma_H(k_c)}_{\sigma_H(k_c)} \\
&= \sigma_0(1+\delta_W+\delta_{\mathrm{QED}}).
\end{aligned}$$

$$\begin{aligned}
d\sigma_S &= d\sigma_0\cdot\delta_S(k_c) = d\sigma_0\cdot f_{LL}(k_\gamma^0<k_c) \\
f_{LL} &= -e^2\int\frac{d^3k_\gamma}{(2\pi)^3 2k_\gamma^0}\left|\frac{p^-}{k_\gamma\cdot p^-}-\frac{p^+}{k_\gamma\cdot p^+}\right|^2,
\end{aligned}$$

In `GRACE-LOOP`the hard photon contribution is performed by the adaptive Monte-Carlo integration `BASES` and the exact matrix elements are generated by `GRACE`.

More efficient way to deal with the large contribution from the collinear regions, $\mathcal{O}(m_e^2/s)$. (of the hard photon radiation) which cancels a large part of the negative contribution from $\delta_{V+S}^{QED}=\delta_V^{QED}+\delta_S$.

Dipole subtraction: The idea is to add and subtract to $d\sigma_H(k_c)$ a function that captures the leading contribution of $d\sigma_H(k_c)$ and which is much easier to integrate. In our case we use the function $d\tilde\sigma_0\otimes f_{LL}$, where $d\tilde\sigma_0$ is derived from the tree-level $d\sigma_0$ but with kinematics taking into account the radiative photon emission. $\otimes$ stands for the phase-space integration of the radiative photon convoluted with 3-body phase-space of the tree-level cross-section.

$$\begin{aligned}
\sigma_{\mathcal{O}(\alpha)} &= \int d\sigma_0\,(1+\delta_V+\delta_S) + \int d\tilde\sigma_0\otimes f_{LL}(k_\gamma^0>k_c) \\
&+ \int\left(d\sigma_H(k_\gamma^0>k_c) - d\tilde\sigma_0\otimes f_{LL}(k_\gamma^0>k_c)\right) \\
&\equiv \sigma_0\,(1+\delta_W) + \underbrace{\int\left(d\sigma_0\,\delta_V^{\mathrm{QED}} + d\tilde\sigma_0\otimes f_{LL}\right)}_{\sigma_A^{QED}} + \underbrace{\int\left(d\sigma_H(k_\gamma^0>k_c) - d\tilde\sigma_0\otimes f_{LL}(k_\gamma^0>k_c)\right)}_{\sigma_B^{QED}}
\end{aligned}$$

The two-dimensional integration over the radiator f_{LL} is performed with the help of the *Good Lattice Point* quasi Monte-Carlo method.

Need automatisation and careful structuring

The Grace System

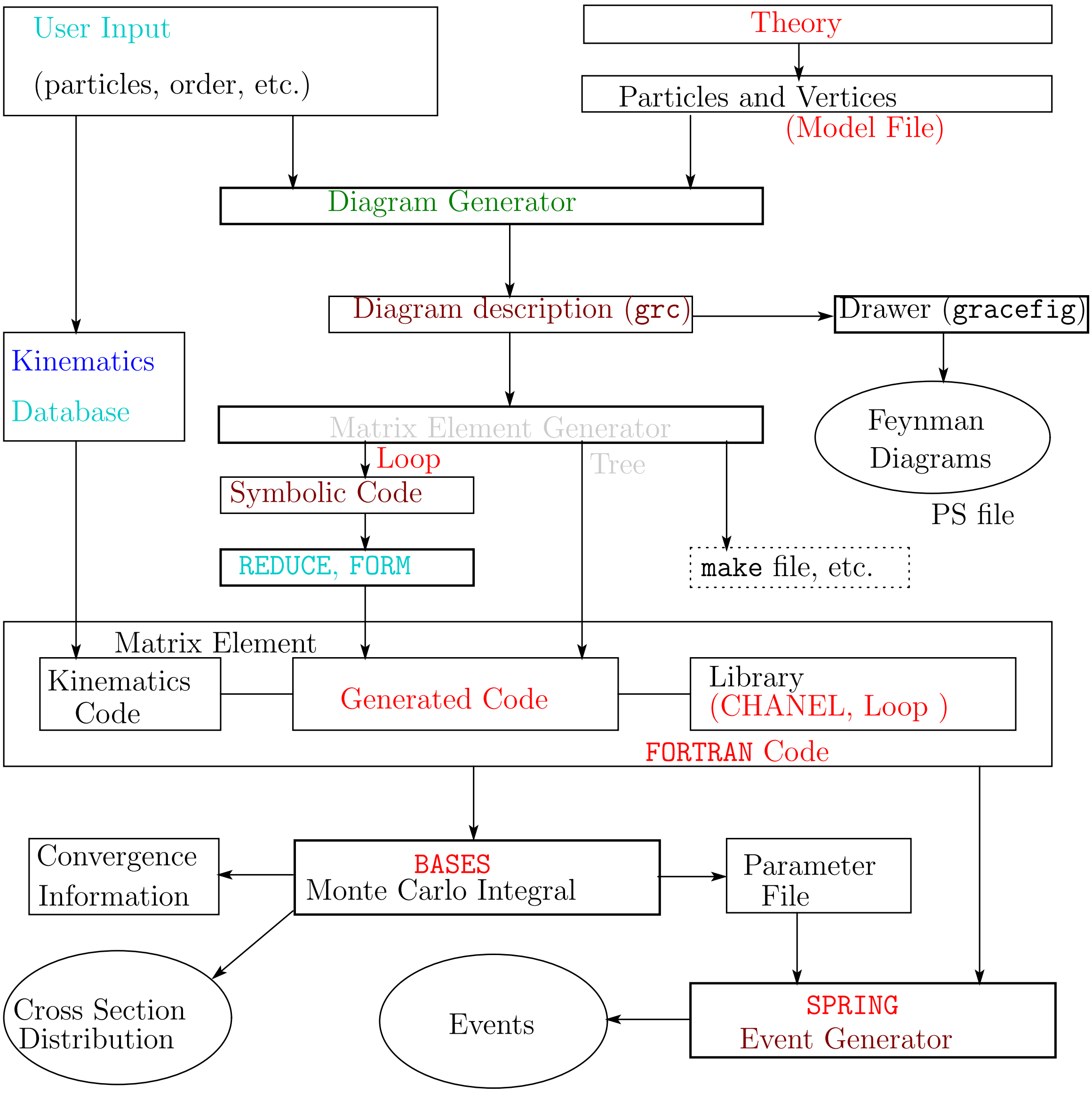

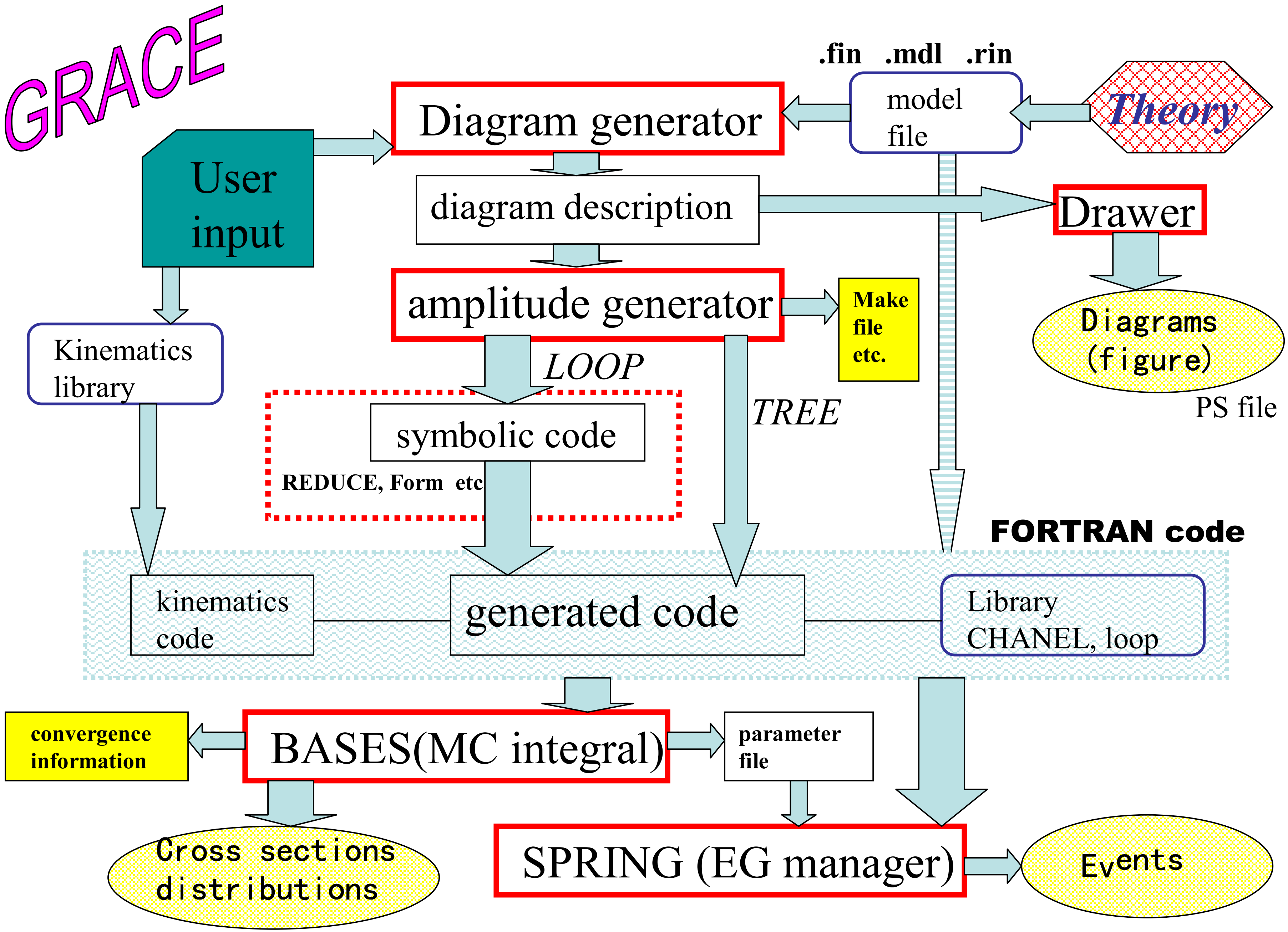
GRACE
.fin .mdl .rin
Diagram generator
model file
Theory
User input
diagram description
Drawer
amplitude generator
Make file etc.
Diagrams (figure)
PS file
Kinematics library
LOOP
TREE
symbolic code
REDUCE, Form etc
FORTRAN code
kinematics code
generated code
Library CHANEL, loop
convergence information
BASES(MC integral)
parameter file
Cross section distributions
SPRING (EG manager)
Events

GRACE/1-loop

On-mass shell renormalization scheme.

use α (Thomson limit), $M_{W,Z,H,f}$

can switch to G_μ scheme (absorbs light fermion logs)

Counterterms are generated automatically

Use dimensional regularization, $n = 4 - 2\epsilon$

Infrared divergence regulated with fictitious photon mass

Symbolic manipulation code based on REDUCE or FORM writes for each diagram

Symbolic manipulation performs: Dirac algebra (taking traces for fermion loops), tensor manipulation in $n = 4 - 2\epsilon$, Feynman parametric integrals, shift momentum... Then Fortran code is generated.

Two libraries for Loop integration: numerical integration with FF package and in-house package for reduction of numerators and numerical integration

Integration over phase space : BASES an adaptative Monte Carlo

System tested in SM at tree-level and at one-loop

Internal checks: ultraviolet divergence, infrared finiteness...

Gauge parameter independence

Comparison with other calculations $2 \rightarrow 2$

Checks on calculation

Checks performed with

1. *One random phase space point*
2. *Full set of diagrams*
3. *Quadruple precision*

Ultraviolet Finiteness
regularise infrared divergence by fictitious photon mass $\lambda = 10^{-15} GeV$
extract term in $C_{UV} = \frac{1}{\epsilon} - \gamma_E + \log 4\pi$
stability of result for different values of $C_{UV} \rightarrow \;\; 30$ *digits precision)*
repeat this test with non-zero non-linear gauge parameters

Infrared finiteness
Regulate infrared divergence in photon exchange diagram with fictitious photon mass λ
Dependence on λ *cancels with the one in soft bremstrahlung*
check independence on $\lambda \rightarrow \;\; 23$ *digits stability*

Gauge parameter dependence
Use non-linear gauge fixing (here $C_{UV} = 0$*)*
Non-trivial check for:
Correct input file: Feynman diagrams, counterterms...
Symbolic manipulation part
Correctness of reduction formulae for tensor integral (including pentagon)

General Non-linear Gauge Fixing

$$\begin{aligned}\mathcal{L}_{GF} &= -\frac{1}{\xi_W}|(\partial_\mu - ie\tilde{\alpha}A_\mu - igc_W\tilde{\beta}Z_\mu)W^{\mu+} \\ &+\xi_W\frac{g}{2}(v+\tilde{\delta}H+i\tilde{\kappa}\chi_3)\chi^+|^2 \\ &-\frac{1}{2\xi_Z}(\partial.Z+\xi_Z\frac{g}{2c_W}(v+\tilde{\varepsilon}H)\chi_3)^2 - \frac{1}{2\xi_A}(\partial.A)^2\end{aligned}$$

FB 87, FB+Chopin 95

Choose t'Hooft-Feynman gauge ($\xi_W = \xi_Z = \xi_A = 1$)

1. *avoid large numerical cancellations*
2. *no need for higher order tensor structure in loop integrals*

Vary parameters $\zeta = (\tilde{\alpha}, \tilde{\beta}, \tilde{\delta}, \tilde{\kappa}, \tilde{\epsilon})$

For each loop graph, g

$$\mathrm{d}\sigma_g = \mathrm{d}\sigma_g(\zeta) = \Re\left(\mathcal{T}_g^{loop}\cdot\mathcal{T}^{tree}\right)$$

Comprehensive checks of NLG parameters independence, for example for only one non-zero parameter, $d\sigma$ polynomial in ζ

$$\mathrm{d}\sigma_g = \mathrm{d}\sigma_g^{(0)} + \zeta\mathrm{d}\sigma_g^{(1)} + \zeta^2\mathrm{d}\sigma_g^{(2)} + \zeta^3\mathrm{d}\sigma_g^{(3)}$$

can reconstruct $d\sigma_g^{(0,1..4)}$ and verify that $d\sigma$ is independent of ζ

$$\mathrm{d}\sigma = \sum_g \mathrm{d}\sigma_g = \sum_g \mathrm{d}\sigma_g^{(0)} \;,$$

$$\mathrm{sum}_i = \frac{\sum_g \mathrm{d}\sigma_g^{(i)}}{\mathrm{Max}_g\left(|\mathrm{d}\sigma_g^{(i)}|\right)} = 0 \;\;,\;\; i=1,2,3\;,$$

set all widths to 0 (choose point away from resonance).

Example of NLG checks

Non-linear gauge parameter checks on $\tilde{\alpha}$ (all other parameters set to zero), for the differential cross section $W^+W^- \to W^+W^-$.

Graph number	$d\sigma_g^{(4)}$	$d\sigma_g^{(3)}$	$d\sigma_g^{(2)}$	$d\sigma_g^{(1)}$	$d\sigma_g^{(0)}$
2			.2335514E+03	.7789374E+03	.5615925E+03
5			-.1721616E+01	-.1171640E+01	.2893256E+01
10			-.4324751E+01	.8649502E+01	-.4324751E+01
13			-.1721616E+01	-.1171640E+01	.2893256E+01
33				.1048909E+01	-.1048909E+01
35				.1048909E+01	-.1048909E+01
			≀		
			≀		
321	-.3606596E+02	.1243056E+03	.6056929E+03	-.1534141E+04	-.4615316E+04
322			-.7411780E-02	.2758337E+00	-.2984030E+01
323			-.2864131E+01	-.2648726E+02	.2935139E+02
324	.2999432E+02	-.1197862E+03	-.1886059E+03	.6165932E+03	-.3381954E+03
325			.7411780E-02	-.1453286E+00	.1379168E+00
326			.7411780E-02	-.1453286E+00	.1379168E+00
327			-.2864131E+01	-.2648726E+02	.2935139E+02
			≀		
			≀		
493		-.1798684E+03	.4305188E+03	-.2277636E+03	-.8935366E+03
494		.8331849E+02	-.2608640E+03	.2717725E+03	-.9422699E+02
495		.8331849E+02	-.2608640E+03	.2717725E+03	-.9422699E+02
496			.1666370E+03	-.3332740E+03	.1666370E+03
498				-.2274438E-01	.2274438E-01
499				-.2274438E-01	.2274438E-01
			≀		
			≀		
741	.3286920E-31	-.6573841E-31	-.2380925E+01	.2380925E+01	.0000000E+00
743				.3853975E+01	-.8927045E+01
749		.6445007E+00	.4734479E+00	.1060865E+01	-.2457305E+01
755				.2853713E+00	-.2853713E+00
758				-.4247529E+01	.4261065E+02
764		.6615728E+01	-.2526752E+02	-.7116714E+01	.7139393E+02
			≀		
			≀		
923				-.1479291E+01	-.1127685E+02
924				-.8424135E+00	.4331788E+03
$Max(\lvert d\sigma_g^{(i)}\rvert)$	36.066	179.87	605.69	1534.1	4615.3
sum_i	.63168E-28	.60757E-29	.44209E-28	.69380E-28	.20116
$\sum_g d\sigma_g^{(i)} / \sum_g d\sigma_g$	.24538E-29	.11771E-29	.28841E-28	.11464E-27	1.0000

Results for $\sum_g d\sigma_g$

$\tilde{\alpha}=0$	928.4382002128633892851311 7*418831577	(input)
$\tilde{\alpha}=1$	928.4382002128633892851311 7*432490231	(input)
$\tilde{\alpha}=-1$	928.4382002128633892851311 7*410983989	(input)
$\tilde{\alpha}=2$	928.4382002128633892851311 7*455347002	(input)
$\tilde{\alpha}=-2$	928.4382002128633892851311 7*411023117	(input)
$\tilde{\alpha}=5$	928.4382002128633892851311 7*695043335	(derived)

Comparisons

• $e^+e^- \to t\bar{t}$

Comparison of the total cross section $e^+e^- \to t\bar{t}$ between GRACE-LOOP and (FLRW)J. Fleischer, A. Leike, T. Riemann, and A. Werthenbach, hep-ph/0302259. The corrections refer to the full one-loop electroweak corrections including hard photon radiation.

$e^+e^- \to t\bar{t}$	GRACE-LOOP	FLRW
$\sqrt{s} = 500$GeV		
tree-level(in pb)	0.5122751	0.5122744
$\mathcal{O}(\alpha)$ (in pb)	0.526371	0.526337
δ (in %)	2.75163	2.74513
$\sqrt{s} = 1$TeV		
tree-level(in pb)	0.1559187	0.1559185
$\mathcal{O}(\alpha)$ (in pb)	0.171931	0.171916
δ (in %)	10.2696	10.2602

• $e^+e^- \to ZH$

Comparison of percentage correction to the total cross section $e^+e^- \to ZH$ between GRACE-LOOP and A. Denner, J. Küblbeck, R. Mertig and M. Böhm, Z. Phys. **C56** (1992) 261 (DKMB).

$e^+e^- \to ZH$	GRACE-LOOP	DKMB
$\sqrt{s} = 500$**GeV** $M_H = 100$**GeV**	**4.15239**	**4.1524**
$\sqrt{s} = 500$**GeV** $M_H = 300$**GeV**	**6.90166**	**6.9017**
$\sqrt{s} = 1000$**GeV** $M_H = 100$**GeV**	$-$**2.16561**	$-$**2.1656**
$\sqrt{s} = 1000$**GeV** $M_H = 300$**GeV**	$-$**2.49949**	$-$**2.4995**
$\sqrt{s} = 1000$**GeV** $M_H = 800$**GeV**	**26.10942**	**26.1094**
$\sqrt{s} = 2000$**GeV** $M_H = 100$**GeV**	$-$**11.54131**	$-$**11.5414**
$\sqrt{s} = 2000$**GeV** $M_H = 300$**GeV**	$-$**12.82256**	$-$**12.8226**
$\sqrt{s} = 2000$**GeV** $M_H = 800$**GeV**	**11.24680**	**11.2468**

• $W^+W^- \to W^-W^+$

Comparison of the total (unpolarised) cross section $W^+W^- \to W^-W^+$ **between** `GRACE-LOOP` and A. Denner and T. Hahn, Nucl.Phys. **B525** (1998) 27; hep-ph/9711302 (DH98). $M_H = 100\text{GeV}$.

$W^+W^- \to W^-W^+$	GRACE-LOOP	DH98
$\boxed{k_c = .05\sqrt{s}}$		
$\sqrt{s} = 2\text{TeV}$		
tree-level(in pb)	77.17067	77.17067
δ (in %)	-21.0135	-21.0135
$\sqrt{s} = 5\text{TeV}$		
tree-level(in pb)	14.2443	14.2443
δ (in %)	-57.1567	-57.1556
$\sqrt{s} = 10\text{TeV}$		
tree-level(in pb)	3.644573	3.644573
δ (in %)	-93.9942	-94.0272
$\boxed{k_c = .5\sqrt{s}}$		
$\sqrt{s} = 2\text{TeV}$		
tree-level(in pb)	77.17067	77.17067
δ (in %)	-17.23988	-17.23989
$\sqrt{s} = 5\text{TeV}$		
tree-level(in pb)	14.24434	14.24434
δ (in %)	-49.9736	-49.9724
$\sqrt{s} = 10\text{TeV}$		
tree-level(in pb)	3.644574	3.644573
δ (in %)	-83.9247	-83.9577

From the Lagrangian to the Feynman Rules

FB and Semenov

```
vector
    A/A: (photon, gauge),
    Z/Z:('Z boson', mass MZ = 91.1875, gauge),
    'W+'/'W-': ('W boson', mass MW = MZ*CW, gauge).
scalar  H/H:(Higgs, mass MH = 115).
```

```
transform A->A*(1+dZAA/2)+dZAZ*Z/2, Z->Z*(1+dZZZ/2)+dZZA*A/2,
    'W+'->'W+'*(1+dZW/2),'W-'->'W-'*(1+dZW/2).
transform H->H*(1+dZH/2), 'Z.f'->'Z.f'*(1+dZZf/2),
    'W+.f'->'W+.f'*(1+dZWf/2),'W-.f'->'W-.f'*(1+dZWf/2).

let pp = { -i*'W+.f',  (vev(2*MW/EE*SW)+H+i*'Z.f')/Sqrt2 },
PP=anti(pp).
```

```
lterm -2*lambda*(pp*anti(pp)-v**2/2)**2
     where
    lambda=(EE*MH/MW/SW)**2/16, v=2*MW*SW/EE .

let Dpp^mu^a = (deriv^mu+i*g1/2*B0^mu)*pp^a +
     i*g/2*taupm^a^b^c*WW^mu^c*pp^b.
let DPP^mu^a = (deriv^mu-i*g1/2*B0^mu)*PP^a
    -i*g/2*taupm^a^b^c*{'W-'^mu,W3^mu,'W+'^mu}^c*PP^b.
lterm DPP*Dpp.
```

Gauge fixing and BRS transformation

```
let G_Z = deriv*Z+(MW/CW+EE/SW/CW/2*nle*H)*'Z.f'.

lterm -G_A**2/2 - G_Wp*G_Wm - G_Z**2/2.

lterm -'Z.C'*brst(G_Z).
```

Output of Feynman Rules with Counterterms !!

```
M$CouplingMatrices = {

  (*------    H  H  ------*)
   C[ S[3], S[3] ] == - I *
{
 { 0 , dZH },
 { 0 , MH^2 dZH + dMHsq }
},
  (*------    W+.f  W-.f  ------*)
   C[ S[2], -S[2] ] == - I *
{
 { 0 , dZWf },
 { 0, 0 }
},
(*------    A  Z  ------*)
   C[ V[1], V[2] ] == 1/2 I / CW^2 MW^2 *
{
 { 0, 0 },
 { 0 , dZZA },
 { 0, 0 }
},


(*------    H  H  H  ------*)
   C[ S[3], S[3], S[3] ] == -3/4 I EE / MW / SW *
{
 { 2 MH^2 , 3 MH^2 dZH -2 MH^2 / SW dSW - MH^2 / MW^2 dMWsq + 2 dMHsq + 2 MH^2 dEE }
},
  (*------    H  W+.f  W-.f  ------*)
   C[ S[3], S[2], -S[2] ] == -1/4 I EE / MW / SW *
{
 { 2 MH^2 , MH^2 dZH + 2 MH^2 dZWf -2 MH^2 / SW dSW - MH^2 / MW^2 dMWsq + 2 dMHsq + 2
},


  (*------    W-.C  A.c  W+  ------*)
   C[ -U[3], U[1], V[3] ] == - I EE *
{
 { 1 },
 { - nla }
},

RenConst[ dMHsq ] := ReTilde[SelfEnergy[prt["H"] -> prt["H"], MH]]
RenConst[ dZH ] := -ReTilde[DSelfEnergy[prt["H"] -> prt["H"], MH]]
RenConst[ dZZf ] := -ReTilde[DSelfEnergy[prt["Z.f"] -> prt["Z.f"],
MZ]] RenConst[ dZWf ] := -ReTilde[DSelfEnergy[prt["W+.f"] ->
prt["W+.f"], MW]]
```

Results: Higgs profile at the LC

$$e^+e^- \rightarrow \nu\bar{\nu}H$$

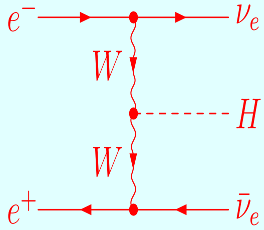

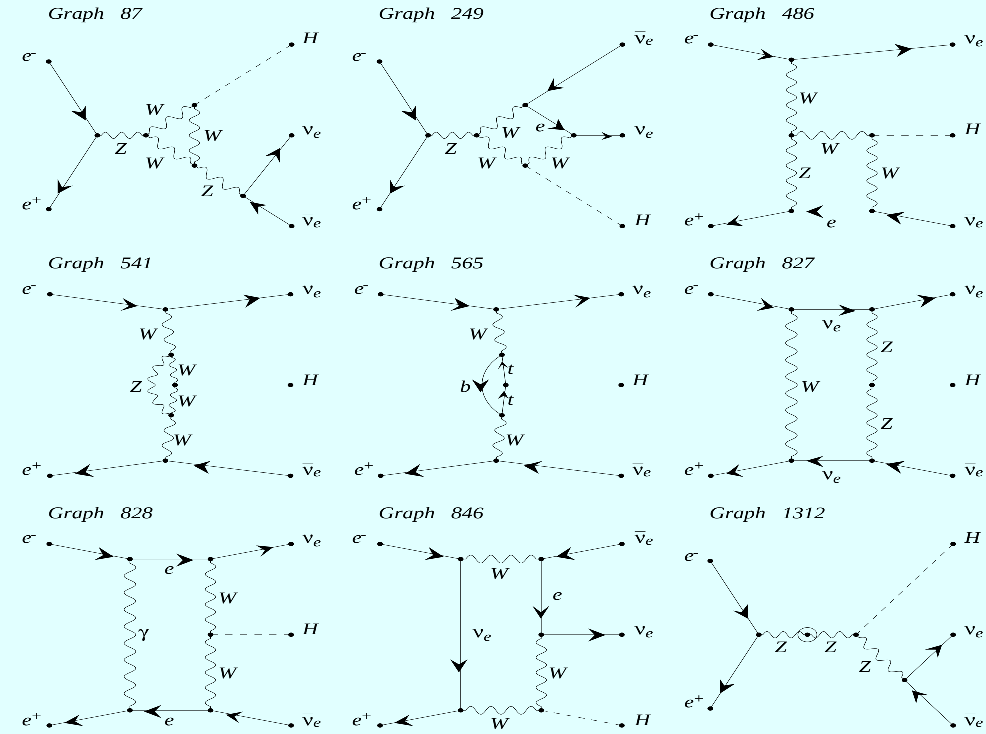

produced by GRACEFIG

interference s and t channel

no QED final state corrections

photon diagrams not GI, extract universal factor (correct in leading terms)

Total $\mathcal{O}(\alpha)$ in α scheme

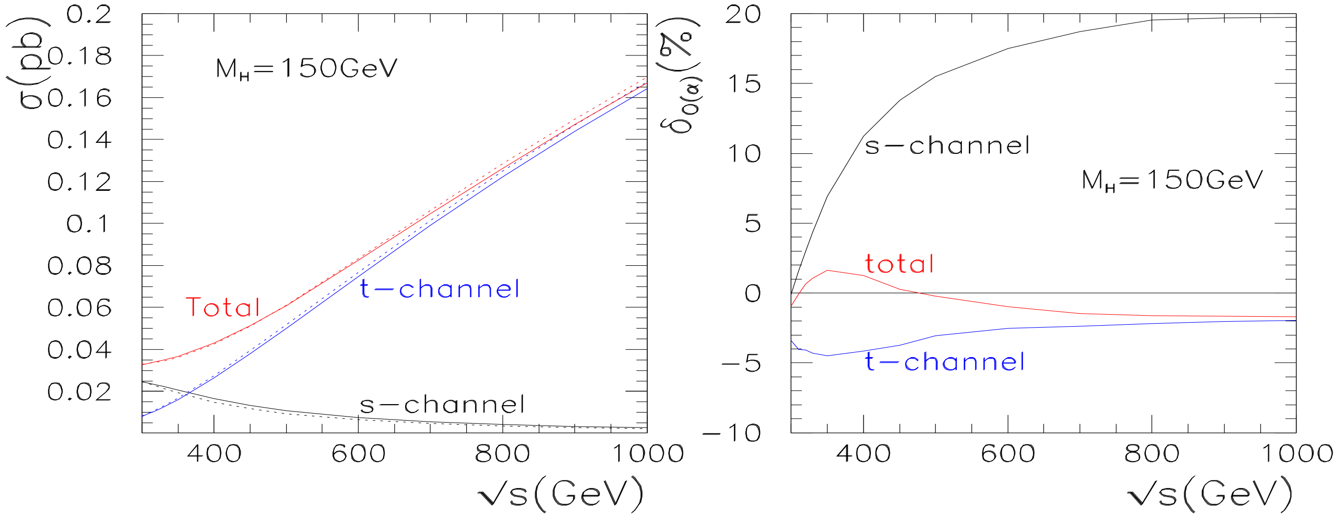

- *Corrections in the s and t-channel are drastically different*
- *in s-channel sharp with energy rise reaching as much $+20\%$*
- *for the total (including WW fusion) and for a light Higgs, full $\mathcal{O}(\alpha)$ correction is rather small: within ± 2*
- *Dependence with Higgs mass shows spikes due to thresholds ($WW, ZZ, t\bar{t}$)*
- *s-channel shows extremely large variations (but overall contribution small and most of this is QED in origin)*
- *correction for the total is moderate (negative) for all Higgs masses at $\sqrt{s} = 500$GeV.*

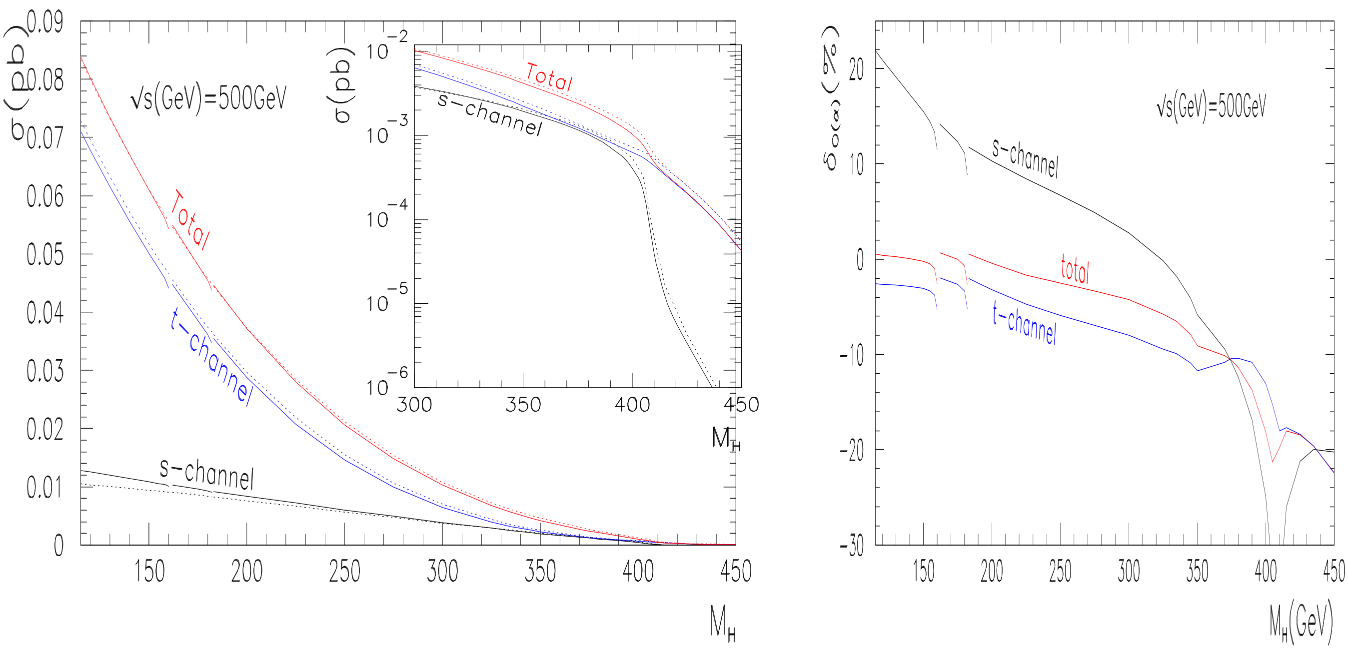

Genuine weak corrections

Extract from the soft+virtual the universal factor for QED ISR

$$\delta^{QED}_{V+S} = \frac{2\alpha}{\pi}\left((L_e - 1)\ln\frac{k_c}{E_b} + \frac{3}{4}L_e + \frac{\pi^2}{6} - 1\right), \qquad L_e = \ln(s/m_e^2)\,,$$

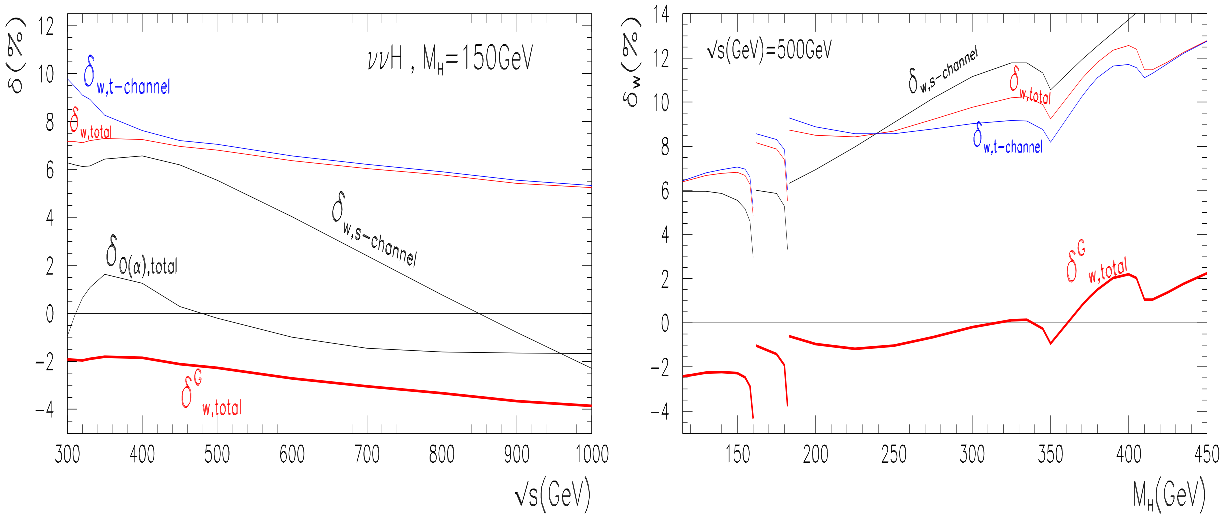

• *The G_μ scheme describes quite well the genuine weak correction for the WW fusion process and hence the total contribution:* $\boxed{|\delta^G_W| \sim 2-4\%}$

• *Especially for light Higgs masses and for the largest cross sections, one can get even closer within* $\boxed{1-2\%}$ *to the genuine weak correction by absorbing the M_t^2 corrections to the HWW vertex:*

$$\delta_{HWW} = -\frac{5\alpha}{16\pi\sin\theta_W^2}\frac{M_t^2}{M_W^2} \sim -1.5\%$$

• *G_μ scheme not appropriate for Higgsstrahlung.*

• *Corrections to Higgs distributions mainly due to QED*

Our calculation confirmed by Denner, Dittmaier, Roth and Weber hep-ph/0302198 and hep-ph/0301189.

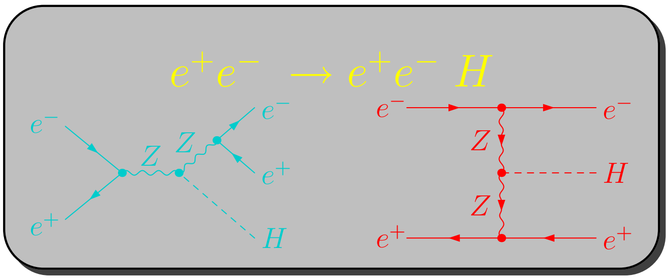

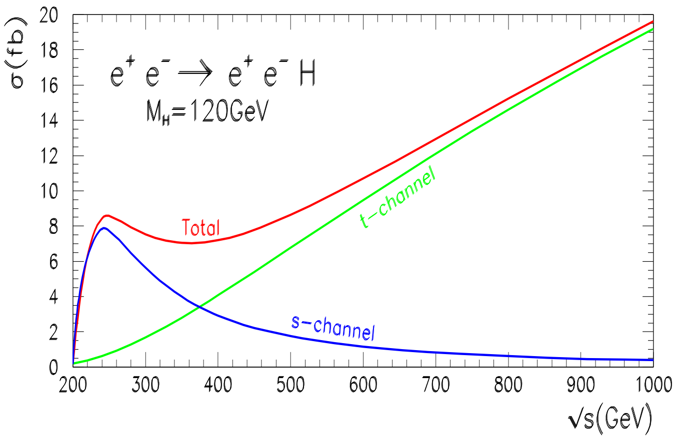

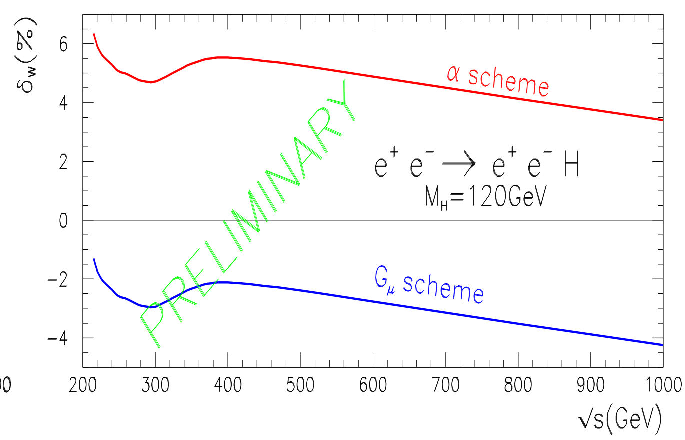

- *results are quite similar to what we have for $\nu\bar{\nu}H$*
- *QED corrections can be extracted exactly* • *genuine weak corrections are of order few per-cent, both in α and G_μ scheme*
- *The G_μ scheme describes quite well the genuine weak correction with* $\boxed{|\delta_W^G| \sim 2-4\%}$

more results on $e^+e^- \longrightarrow e^+e^- H$ soon

$$e^+e^- \to t\bar{t}H$$

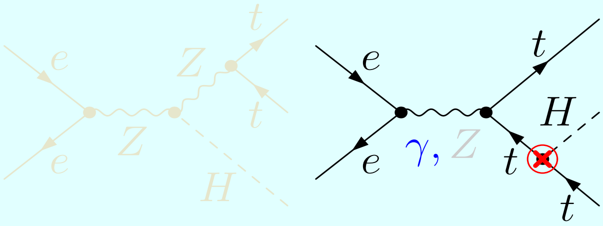

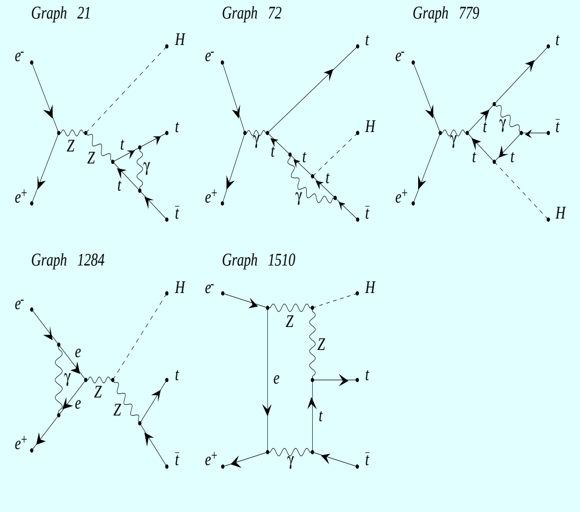

Subset of QED corrections produced by GRACEFIG

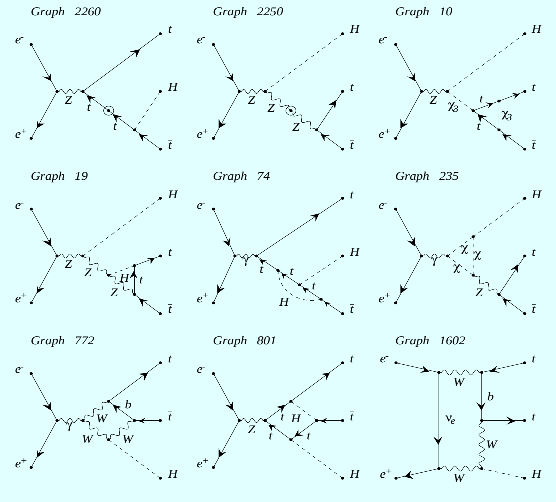

produced by GRACEFIG

QED Corrections genuine electroweak corrections

- *QED corrections form a gauge invariant subset. Which moreover can be split into Initial (Q_e^2) Final (Q_t^2) Interference (Q_eQ_t)*
- *QCD corrections: These can be extracted from the QED final state corrections*

$$\alpha Q_t^2 \to C_F\ \alpha_s(\mu)$$

$$\delta_{\mathcal{O}(\alpha_s)} = C_F\ \alpha_s(\mu)\ \Delta_s, \qquad C_F = 4/3.$$

Cross section dominated by photon exchange.
Highest yield about 2fb at $\sqrt{s} = 700 - 800$GeV.
with 1ab^{-1} statistical accuracy about 2%.

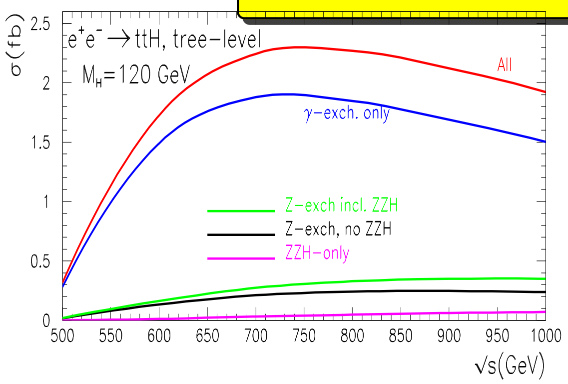

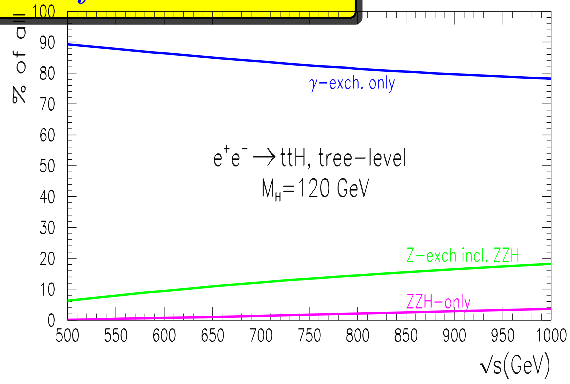

Radiative Corrections

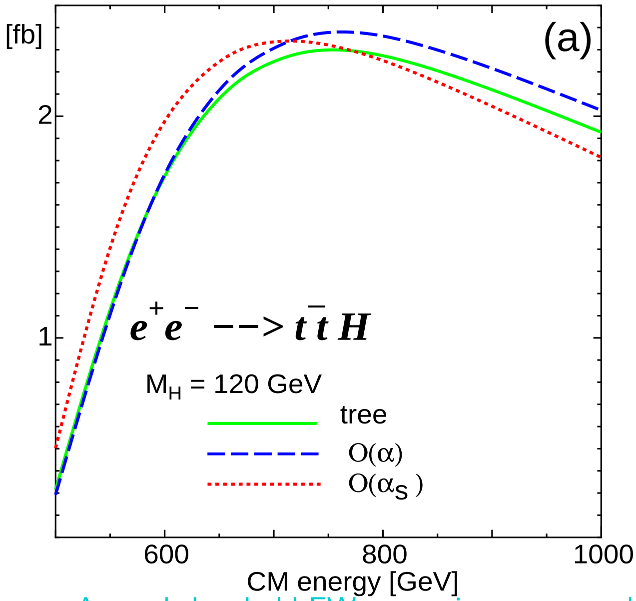

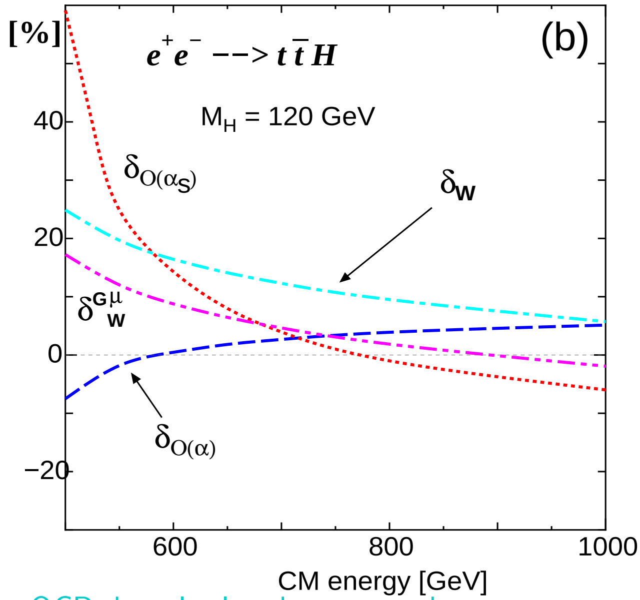

Around threshold EW corrections swamped by QCD, but slowly take over as the energy increases.

At energies around the peak (where it matters) the $\mathcal{O}(\alpha)$ larger than QCD and therefore a good chance to see the EW effects. QCD corrections here have negligible scale dependence.

The total genuine weak corrections are not small, being largest around threshold ($\sim +25\%$ at $\sqrt{s} = 500$GeV $M_H = 120$GeV) and decrease monotonically as the energy increases.

In the G_μ scheme and for $\sqrt{s}$ at peak (and up to $1TeV$) genuine weak corrections are modest (5% to -2%)but must be taken into account (applies for $M_H = 180$GeV also)

Taking into account the leading correction to the $t\bar{t}H$ vertex $y_{t\bar{t}H}$

$$y_{t\bar{t}H} = y^0_{t\bar{t}H}\left(1 + \frac{7}{2}\frac{G_\mu M_t^2}{8\pi^2\sqrt{2}}\right)$$

In the total cross section this only accounts for about 2.2% weak correction.

- Our calculation completely confirmed by Denner, Dittmaier, M. Roth and M.M. Weber, hep-ph/0307193 but does not agree so well with You Yu, Ma Wen-Gan, Chen Hui, Zhang Ren-You, Sun Yan-Bin and Hou Hong-Sheng, hep-ph/0306036 at high energies.

$$e^+e^- \rightarrow ZHH$$

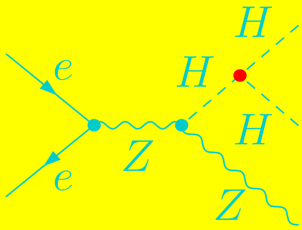

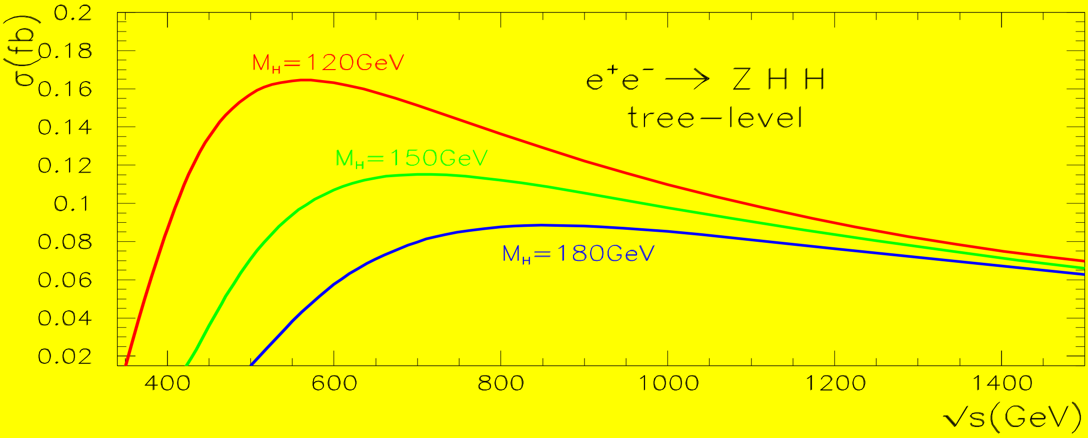

Cross sections are small, max ~ 0.2fb.

with 1ab^{-1} and use of NN (neural network) hope to measure total cross section at 10%.

Very fast increase of the total cross section after threshold and moderately fast after.

Selection of 1-Loop graphs

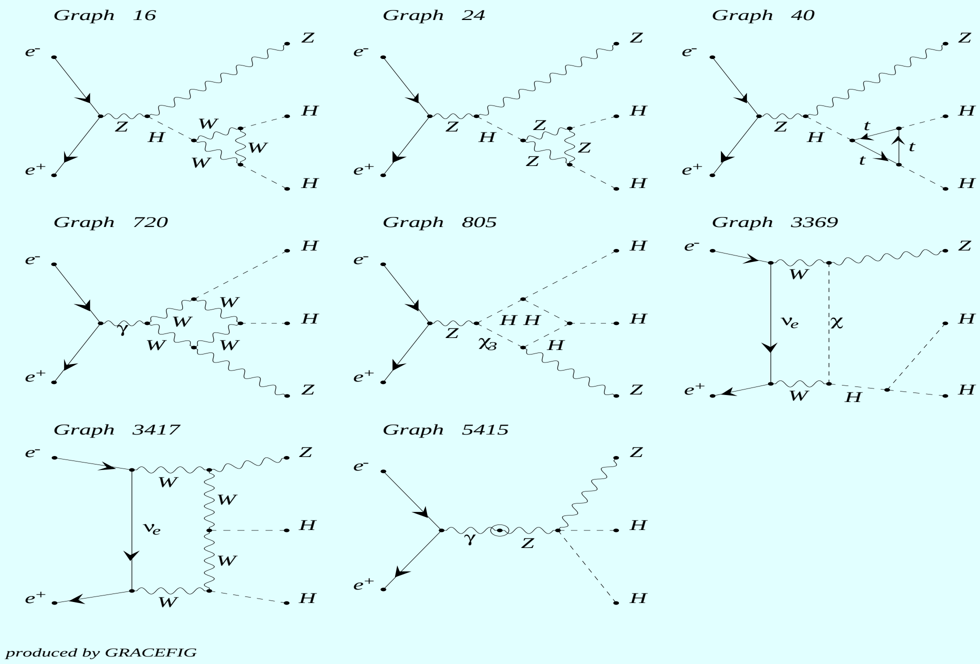

QED corrections easy to extract.

$\sqrt{s}$ [GeV]	δ_{QED} [%]
400	-18.83
600	-3.60
800	1.53
1000	4.31
1500	8.04

QED CORRECTIONS

Quite large at threshold, moderate for energies of interest, rise with energy. This can be explained by the *radiative return*

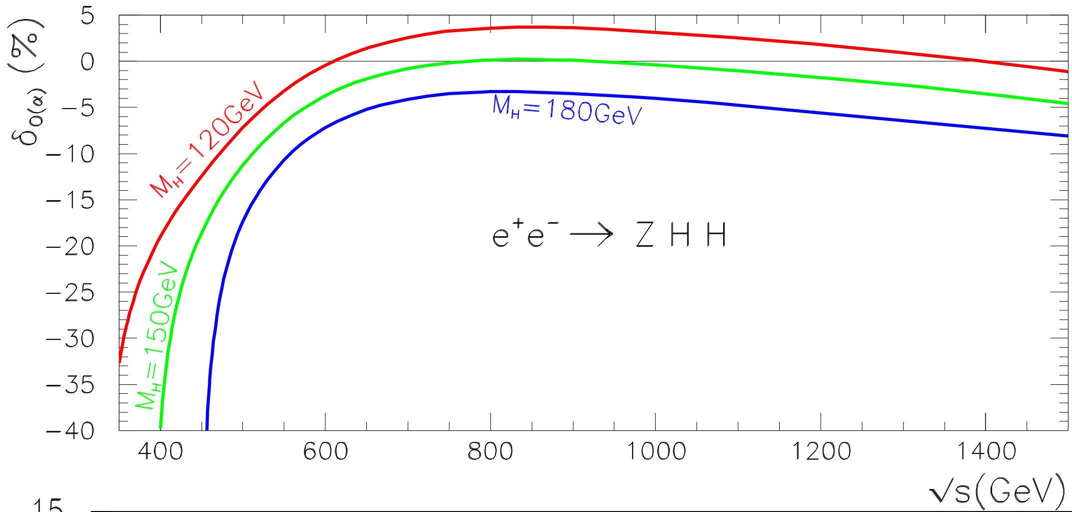

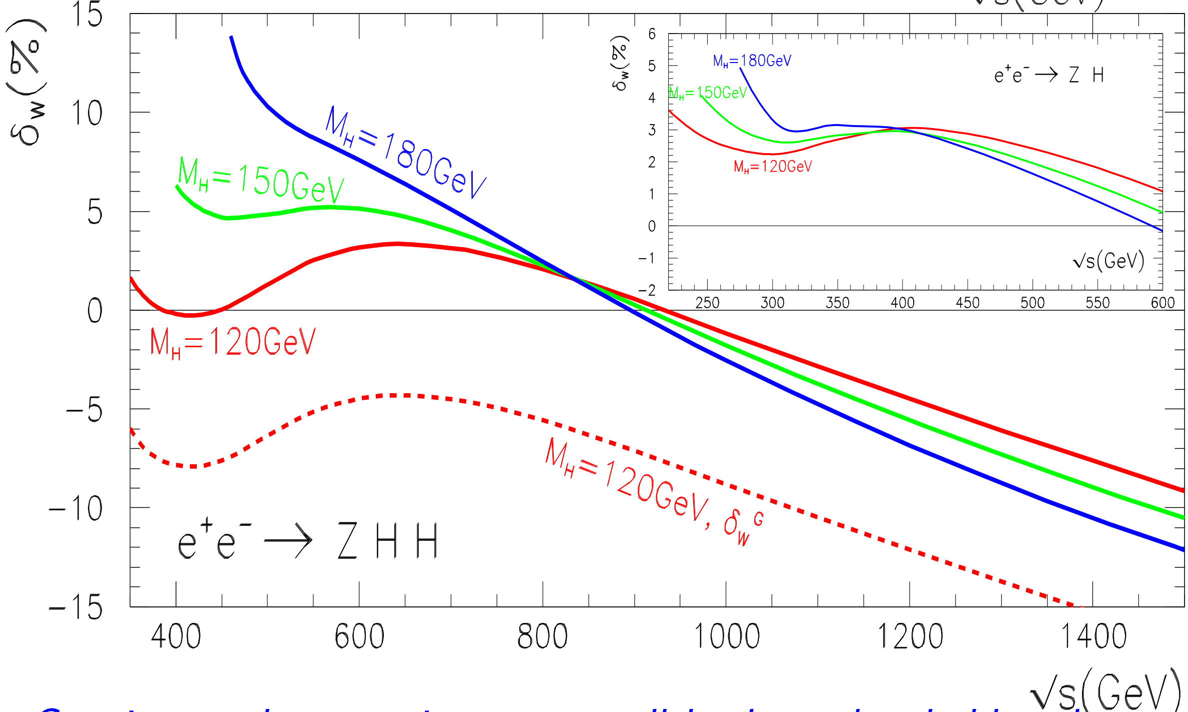

- *Genuine weak corrections are small both at threshold and at energies around peak, never more than* $|\sim 4\%|$.

This can be considered as negligible considering the foreseen experimental precision $> 10\%$). *This is true both in* α *and* G_μ *scheme)*

- *They grow large at high energies* (~ 1.5 *TeV* $\to -10\%$)

- *Note the spoon-like behaviour is typical of* $s-$*channel* ZH *production mechanisms.*

Like in ZH G_μ *scheme not so appropriate at high energies.*

M_{HH} **distribution**

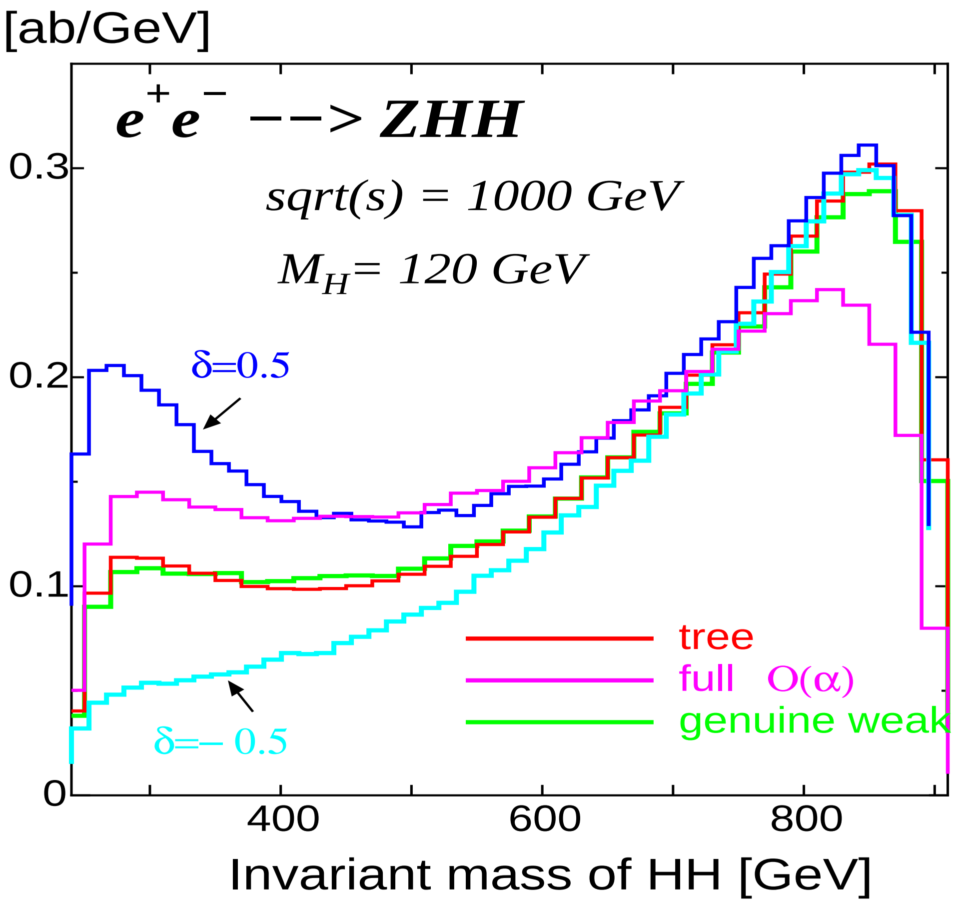

M_{HH} is a good discriminator for picking up the HHH or rather $H^* \to HH$ vertex (FB 95)

at $\sqrt{s} = 1$TeV ($M_H = 120$GeV) $\mathcal{O}(\alpha) \sim 3\%$ but $\delta_W \sim -1$, but $\mathcal{O}(\alpha)$ not uniformly distributed.

genuine weak do not sensibly change the distribution

one could in principle interpret disentangle the effect of an anomalous HHH vertex or an unconventional Higgs potential

Summary ZHH

♡ *If cross sections are not going to be measured more precisely than about 10% than it may be sufficient to only include the initial state radiation for precision measurements on both the cross section and the most promising distribution.*

♠ Our results agree with those of the Chinese group: Zhang Ren-You, Ma Wen-Gan, Chen Hui, Sun Yan-Bin, Hou Hong-Sheng, hep-ph/0308203. there is only a some small disagreement for high energies (same problem but in worse occurred with $e^+e^- \to t\bar{t}H$).

A surprise .....

MicrOMEGAs

a code for the calculation of the relic density in a general supersymmetric model

by
Geneviève Bélanger, Fawzi Boudjema, Alexander Pukhov and Andrei Semenov

«O atomes intelligents, dans qui l'Etre éternel s'est plu à manifester son adresse et sa puissance, vous devez sans doute goûter des joies bien pures sur votre globe : car, ayant si peu de matière...,
Voltaire, Micromegas, chapitre septième, conversation avec les hommes

Introduction

MicrOMEGAs is a code written in C for the calculation of the relic density in supersymmetry. It also calls some external FORTRAN functions. All annihilation processes as well as co-annihilation processes are calculated exactly through a supersymmetric version of CompHEP. Co-annihilation processes include any type of slepton, squark, possible chargino or next to lightest neutralino as well as a gluino. By default the lightest neutralino is assumed to be the LSP, but the user can set any supersymmetric particle (not including Higgses!) to be the LSP, in particular a sneutrino.
All in all we have included about 2800 processes not counting charge conjugate states. Care is taken to deal with resonances (in particular for the Higgs resonances) and thresholds. The present version uses FeynHiggs to calculate the Higgs masses and Hdecay to include important QCD corrections to the width and partial widths of the Higgses. All Yukawa effects are included. MicrOMEGAs can run by providing an unconstrained set of soft SUSY parameters at the electroweak scale. In the present version, a mSUGRA model can be entered though the Isajet interface however any other RGE code can be used. Many constraints can be applied, apart from the present direct limits on the masses of the supersymmetric particles, we provide routines for the muon g-2, b->s \gamma and Delta rho.
We also provide a sample file to be used for scans over a set of parameters as in mSUGRA. It is also possible to view the contributions of different channels to the relic density.

System requirements: C compiler, Fortran compiler, 500 kb of disk space for download, a minimum of 10Mb as working space.
Tested on: Dec Alpha, Silicon Graphics and Linux (Red Hat,Suse), SunOS and HP-UX .

Current version: micromegas_1.1.1 (23 August 2002)
Changes from version 1.0:
(1st version: micromegas_1.0, december 2001)

Shortcomings to be included in next versions:

- Although the program consists of about more 2800 processes (not counting charge conjugate related processes, etc), only tree-level processes are included. Missing are one-loop processes with 2\gamma and 2 gluons in the final state. For the relic density these are negligible.
- Radiative corrections to neutralino and chargino masses are not implemented in the current version.
- A new routine for b->s\gamma which includes NLO effects and large tgb effects will be included soon.

Summary

Within the 12 past months considerable progress in the calculations of loop corrections to the Higgs production processes at the LC

These calculations are well under control and show the power of automatic codes for handling $2 \to 3$ processes in the SM

It is important for these codes to have stringent internal checks, $e.g$ gauge invariance,..

The genuine electroweak corrections to the cross sections are small but for most processes still important for precision measurements

QED corrections can be large, but these can be easily resummed, QEDPS, structure functions,..

application a susy à une boucle: en cours

encore plus d'automatisation en très bonne voie

Applications QCD:?

back up transparency for ttH

$\sqrt{s}$	M_H(GeV)	σ_{tree}(fb)	$\sigma_{\mathcal{O}(\alpha_s(M_t))}$(fb)	$\delta_{\mathcal{O}(\alpha_s(M_t))}(\%)$	$\delta_{\mathcal{O}(\alpha_s(\sqrt{s}))}(\%)$
600 GeV	120	1.7293 ± 0.0003	1.977 ± 0.001	14.3	12.4
	180	0.33714 ± 0.00004	0.4383 ± 0.0004	30.0	26.0
800 GeV	120	2.2724 ± 0.0005	2.250 ± 0.002	-1.0	-0.8
	180	1.0672 ± 0.0003	1.0856 ± 0.0007	1.7	1.4
1 TeV	120	1.9273 ± 0.0005	1.812 ± 0.003	-6.0	-4.9
	180	1.1040 ± 0.0003	1.049 ± 0.001	-5.0	-4.1

(A) We choose the renormalization scale μ of the QCD coupling α_s at $M_t = 174$ GeV with $\alpha_s(M_t) = 0.10754$.
(B) We take $\mu = \sqrt{s}$ with $\alpha_s = 0.09330$ at $\sqrt{s} = 600$ GeV, $\alpha_s = 0.09051$ at $\sqrt{s} = 800$ GeV and $\alpha_s = 0.08847$ at $\sqrt{s} = 1$TeV.

Large corrections at threshold (Coulomb corrections)

At the peak (where it matters) QCD corrections are small and with even smaller scale dependence back up transparency for ttH

Purely QED Corrections

M_H (GeV)	$\sqrt{s}$ (GeV)	$\sigma^{QED}_{V+S,Full}$(fb) ($\sigma^{QED}_{hard,Full}$(fb))	$\sigma^{QED}_{V+S,Init.}$ (fb)	$\sigma^{QED}_{V+S,Fin.}$ (fb)	$\sigma^{QED}_{V+S,Int.}$ (fb)	δ^{QED} (%)	δ_W (%)
120							
	600	-2.6092 (2.3333)	-2.557	-0.012	-0.043	-16.0	16.5
	800	-3.6667 (3.5391)	-3.516	-0.055	-0.099	-5.6	9.5
	1000	-3.2622 (3.2507)	-3.086	-0.071	-0.109	-0.6	5.8
180							
	600	-0.50490 (0.41839)	-0.4985	0.0056	-0.0072	-25.7	18.4
	800	-1.7120 (1.5975)	-1.651	-0.020	-0.043	-10.7	9.1
	1000	-1.8589 (1.8048)	-1.768	-0.035	-0.058	-4.9	4.4

$\sigma^{QED}_{V+S,Full}$ corresponds to the cross section for the full one-loop QED virtual and soft bremsstrahlung with $k_c = 0.001$GeV. $\sigma^{QED}_{V+S,Init.}$ extracts the initial state radiation. $\sigma^{QED}_{V+S,Fin.}$ gives the final state QED correction whereas $\sigma^{QED}_{V+S,Int.}$ is the initial-final QED interference contribution. We also give $\sigma^{QED}_{hard,Full}$ which is the full hard photon radiation cross section. All cross sections are in fb.

Large (negative) QED corrections at low energies (ISR)

The genuine weak corrections, δ_w at threshold in the α scheme are large

Back up transparency, ZHH

$\sqrt{s}$ (GeV)	M_H (GeV)	σ_{tree} (fb)	$\sigma_{\mathcal{O}(\alpha)}$ (fb)	$\delta_{\mathcal{O}(\alpha)}$ [%]
	115	*0.17493(2)*	*0.1629(2)*	*−6.9(1)*
		0.17491(2)	0.16282(2)	−6.91(1)
500	150	*0.071834(6)*	*0.06357(6)*	*−11.50(7)*
		0.071830(5)	0.063529(9)	−11.59(9)
	200	*0.49611(3) · 10^−3*	*0.3329(2) · 10^−3*	*−32.90(4)*
		$0.49606(4) \cdot 10^{-3}$	$0.332(3) \cdot 10^{-3}$	−33.0(6)
	115	*0.14156(3)*	*0.1471(3)*	*+3.9(2)*
		0.14155(1)	0.14705(2)	+3.89(1)
800	150	*0.11363(2)*	*0.1135(2)*	*−0.1(2)*
		0.11362(1)	0.11353(1)	−0.08(7)
	200	*0.07246(1)*	*0.0705(1)*	*−2.7(1)*
		0.072454(7)	0.07044(1)	−2.78(1)
	115	*0.07119(2)*	*0.0704(3)*	*−1.1(4)*
		0.07118(1)	0.07058(2)	−0.85(3)
1500	150	*0.06684(2)*	*0.0634(2)*	*−5.1(3)*
		0.06683(1)	0.06359(2)	−4.86(3)
	200	*0.06165(1)*	*0.0569(2)*	*−7.7(3)*
		0.061644(6)	0.05707(2)	−7.42(3)
	115	*0.05021(1)*	*0.0473(2)*	*−5.8(4)*
		0.05021(1)	0.04773(2)	−4.95(4)
2000	150	*0.04812(1)*	*0.0435(2)*	*−9.6(4)*
		0.048119(5)	0.04387(3)	−8.83(7)
	200	*0.04630(1)*	*0.0408(2)*	*−11.9(4)*
		0.046300(4)	0.04115(3)	−11.13(6)

Comparison with Zhang Ren-You et al.,

hep-ph/0308203 v3 *For the c.m. energy $\sqrt{s} = 500GeV$, which is the most favorable colliding energy for HHZ production with intermediate Higgs boson mass, the relative correction decreases from −5.3% to −11.5%* as m_H *increases from 100 to 150 GeV. For the range of the c.m. energy where the cross section is relatively large, the genuine weak relative correction is small, less than 5%.*

hep-ph/0308203 v1 *for the c.m. energy $\sqrt{s} = 500GeV$, which is the most favorable colliding energy for HHZ production with intermediate Higgs boson mass, the relative correction decreases from −5.3% to −32.9% as m_H increases from 100 to 200 GeV.*